

Concatenated Turbo/LDPC codes for deep space communications: performance and implementation

*Original*

Concatenated Turbo/LDPC codes for deep space communications: performance and implementation / Condo, C.. - ELETTRONICO. - (2013), pp. 1-6. (SPACOMM 2013 Mestre 21-26 Aprile 2013).

*Availability:*

This version is available at: 11583/2507647 since:

*Publisher:*

International Academy, Research and Industrial Association (IARIA)

*Published*

DOI:

*Terms of use:*

This article is made available under terms and conditions as specified in the corresponding bibliographic description in the repository

*Publisher copyright*

(Article begins on next page)

# Concatenated Turbo/LDPC Codes for Deep Space Communications: Performance and Implementation

Carlo Condo

Department of Electronics and Telecommunications  
Politecnico di Torino  
Torino, Italy  
carlo.condo@polito.it

**Abstract**—Deep space communications require error correction codes able to reach extremely low bit-error-rates, possibly with a steep waterfall region and without error floor. Several schemes have been proposed in the literature to achieve these goals. Most of them rely on the concatenation of different codes that leads to high hardware implementation complexity and poor resource sharing. This work proposes a scheme based on the concatenation of non-custom LDPC and turbo codes that achieves excellent error correction performance. Moreover, since both LDPC and turbo codes can be decoded with the BCJR algorithm, our preliminary results show that an efficient hardware architecture with high resource reuse can be designed.

**Keywords**—LDPC; turbo; concatenation; deep space

## I. INTRODUCTION

The world of communications is characterized by a continuous strive for better performance: communication systems are usually pushed towards higher throughput, lower Bit-Error-Rate (BER) and lower power consumption with every generation. A particular application is deep space communications: due to the limited number of complete developments, their evolution in this domain is slower than in other application fields. Moreover, their requirements and constraint can differ substantially from all other communication environments. Transmission between spacecrafts and Earth are supposed to be sporadic events, but the limited amounts of available power and the long distances make failed reception, and consequent retransmission, an unacceptable event. For this reason, deep space missions do not require a high throughput, while at the same time they demand very strict BER and frame-error-rate (FER) performance. The Consultative Committee for Space Data Systems (CCSDS) suggests a set of rules (a *de facto* standard) for all space-related communication systems. In [1] four channel coding schemes are described, while in [2] the considered channel coding options are assembled into application-wise FEC schemes. Deep space exploration requires the use of powerful error correction codes, such as turbo codes [3], lower rate low-density-parity-check (LDPC) codes [4] and concatenated Reed-Solomon (RS) and convolutional codes. Various works have proposed deep space FEC schemes, also using codes that are different from those suggested in [1]: from custom-constructed single codes [5] to more complex concatenated schemes [6]. Concatenation between different codes has been frequently considered in order to improve performance. “Guaranteed-performance-codes” like RS or BCH codes are

often used as Outer Codes (OCs) thanks to their measurable error correction capabilities, and joined to Inner Codes (ICs) such as convolutional or LDPC, used in WiMAX and DVB-S2. The same RS+convolutional FEC scheme devised in [2] allows these codes to rival with the more powerful LDPC and turbo codes. However, concatenation comes at a usually high implementation cost: decoding support for sometimes very different codes must be provided, increasing area and power consumption. Low-complexity decoders have been designed for many codes [7], [8] but steps have been recently taken towards flexibility, with area efficient multi-code decoders [9], [10].

This paper presents a deep space oriented FEC scheme by serial concatenation of LDPC and turbo codes. Section II describes how, through a particular representation of the LDPC parity check matrix, both kinds of codes can be decoded with the same algorithm, allowing very low-cost implementation of a joint decoder. The FEC scheme is described in detail in Section III. Performance of the concatenated scheme is compared with the standard requirements in Section IV, together with a set of recent works both on deep space communications and on concatenated codes. Finally, an estimation of the complexity of decoder supporting both codes is made in Section V.

## II. TURBO AND LDPC DECODING ALGORITHMS

Convolutional Turbo Codes (or CTCs) are obtained as the parallel concatenation of two constituent Convolutional Code (CC) encoders. Consequently, also the decoder is made of two different parts, called Soft-In-Soft-Out (SISO) or Maximum-A-Posteriori (MAP) decoders, and connected by an interleaver  $\Pi$  and a de-interleaver  $\Pi^{-1}$ . Each MAP decoder implements the BCJR algorithm [11], which produces extrinsic metrics from *a priori* information. Representing the constituent CC as a trellis, let us define  $k$  as a trellis step and  $u$  as an uncoded symbol. Each decoder computes  $\lambda_k[u] = \lambda_k^{apo}[u] - \lambda_k^{apr}[u] - \lambda_k[\mathbf{c}^u]$  where  $\lambda_k^{apo}[u]$  is the a-posteriori information,  $\lambda_k^{apr}[u]$  is the *a priori* information and  $\lambda_k[\mathbf{c}^u]$  is the systematic component of the intrinsic information. The a-posteriori information is obtained as follows:

$$\lambda_k^{apo}[u] = \max_{e:u(e)=u}^* \{b(e)\} - \max_{e:u(e)=\tilde{u}}^* \{b(e)\} \quad (1)$$

where  $\tilde{u} \in \mathcal{U}$  is an uncoded symbol taken as a reference (usually  $\tilde{u} = \mathbf{0}$ ) and  $u \in \mathcal{U} \setminus \{\tilde{u}\}$  with  $\mathcal{U}$  the set of uncoded

symbols;  $e$  is a trellis transition and  $u(e)$  is the corresponding uncoded symbol. Following the Max-Log-MAP approximation [12], for a small BER degradation the  $\max^*\{x_i\}$  function becomes  $\max\{x_i\}$ . The term  $b(e)$  in (1) can consequently be defined as:

$$b(e) = \alpha_{k-1}[s^S(e)] + \gamma_k[e] + \beta_k[s^E(e)] \quad (2)$$

$$\alpha_k[s] = \max_{e: s^E(e)=s} \{ \alpha_{k-1}[s^S(e)] + \gamma_k[e] \} \quad (3)$$

$$\beta_k[s] = \max_{e: s^S(e)=s} \{ \beta_{k+1}[s^E(e)] + \gamma_k[e] \} \quad (4)$$

$$\gamma_k[e] = \lambda_k^{appr}[u(e)] + \lambda_k[c(e)] \quad (5)$$

where  $s^S(e)$  and  $s^E(e)$  are the starting and the ending states of  $e$ ,  $\alpha_k[s^S(e)]$  and  $\beta_k[s^E(e)]$  are the forward and backward metrics associated to  $s^S(e)$  and  $s^E(e)$  respectively, while  $\lambda_k[c(e)]$  is the channel intrinsic information.

LDPC codes are identified by a sparse parity check matrix  $\mathbf{H}$ , of size  $M \times N$ . A received codeword must satisfy all the parity checks (rows) of  $\mathbf{H}$ , i.e.  $\mathbf{H} \cdot x' = 0$ , where  $x$  is the codeword of length  $N$ . Different decoding approaches are possible, depending on the graph representation of  $\mathbf{H}$ : the classical approach defines a bipartite graph with  $N$  Variable Nodes (VNs) and  $M$  Check Nodes (CNs), and edges between  $VN_i$  and  $CN_j$  if a nonzero entry is present in column  $i$  and row  $j$  of  $\mathbf{H}$ . Layered decoding [13] on the contrary, sees  $\mathbf{H}$  as a multipartite graph composed of different layers of parity checks: this scheduling allows to exploit faster convergence thanks to multiple updates of the bit error probabilities within a single iteration.

Calling  $\lambda[c]$  the Logarithmic Likelihood Ratio (LLR) of symbol  $c$  and, for column  $k$  in  $\mathbf{H}$ , bit LLR  $\lambda_k[c]$  is initialized to the corresponding received soft value. These are the VN-to-CN messages. The following operations are executed for all parity constraints  $l$  in a given layer, and reiterated up to the desired level of reliability:

$$\Delta\lambda_{lk}[c] = \lambda_k[c] - \Lambda_{lk}^{appr} \quad (6)$$

$$\lambda_k[c] = \Delta\lambda_{lk}[c] + \Lambda_{lk}^{apo} \quad (7)$$

where  $\Lambda_{lk}^{apo}$  is the CN-to-VN message, namely the updated version of  $\Lambda_{lk}^{appr}$ , that is initialized to 0, and stored for the next iteration. Several exact and approximated algorithms have been proposed to calculate  $\Lambda_{lk}^{apo}$ : the most common algorithm used in LDPC decoding is the *Belief Propagation* (BP) algorithm, of which one of the most used approximations is the *min-sum* and its variations [14].

It can be clearly seen that LDPC and turbo decoding processes share many characteristics. Both of them are iterative, rely on soft information, are usually implemented in their logarithmic form, while commonly being represented through special kinds of graphs. A particularly interesting exploitation of these characteristics has been proposed in [15]. Every row of  $\mathbf{H}$  is seen as a turbo code with trellis length equal to the row weight: a direct link between turbo and LDPC codes is drawn, and turbo decoding algorithms can be applied to LDPC codes

with minor adjustments. The BCJR-based LDPC decoding relies on the fact that binary LDPC codes have a 2-state trellis: state metrics can consequently be expressed as differences  $\Delta\alpha[c]$  and  $\Delta\beta[c]$ , reducing the quantization noise. Defining  $\Phi(x, y) = \max(x, y) - \max(x+y, 0)$  and considering the Max-Log-MAP approximation [16], the CN-to-VN message update becomes:

$$\Lambda_{lk}^{apo} = \Phi(\Delta\alpha_k[c], \Delta\beta_k[c]) \quad (8)$$

$$\Delta\alpha_k = \Phi(\Delta\alpha_{k-1}[c], \Delta\lambda_{lk}[c]) \quad (9)$$

$$\Delta\beta_k = \Phi(\Delta\beta_{k+1}[c], \Delta\lambda_{lk}[c]) \quad (10)$$

where  $\Delta\alpha[c]$  and  $\Delta\beta[c]$  at the edge of the trellis are initialized as the minimum value of the dynamic range.

### III. PROPOSED FEC SCHEME

In the CCSDS recommended standard [17] transmission data rates of up to 2.048 Mb/s are foreseen for the next missions, while FEC schemes must be able to guarantee bit error floors not higher than  $10^{-9}$ . The need for effective coding schemes, alongside simple decoding algorithms, makes code concatenation one of the smartest solutions. The powerful Turbo and LDPC codes have been considered for concatenation before ([18]) but the low level of details provided and the unsatisfying results leave room for further investigation.

The devised FEC scheme is shown in Fig. 1: an LDPC code is serially concatenated to a turbo code. The outer encoder encodes the input bits, and the resulting codeword is used as input for the inner encoder. Being responsible of the first, rough decoding, the IC should work well also in presence of a large number of errors. Since turbo codes have better performance than LDPC at low SNR [19], they have been chosen as IC. On the contrary, receiving the updated information from the inner decoder, the OC decoder, that is an LDPC code, can fully exploit its deep waterfall region and low error floor. An interleaver scrambles the output of the OC encoder before the second encoding, while the inverse function is inserted between the decoders. Since, depending on the rate and characteristics of the chosen codes, the block sizes may not be compatible, an optional padding block has been placed after the interleaver: zeros are added to the scrambled codeword to fit the required number of bits. This reduces the coding efficiency but allows for flexible concatenation. The padding bits are removed after the IC decoding, before the deinterleaver.

The decoding process starts in the IC decoder, which performs up to  $Iter_{in}$  iterations. After  $Iter_{in}$  the codeword is stripped of the padding bits, descrambled and passed to the OC decoder. Both turbo and LDPC code decoding algorithms involve soft information: while the IC decoder receives measures of bit error probabilities from the channel estimator, the OC decoder must rely on the metrics updated by the IC decoder. In particular, the LDPC decoder receives as intrinsic information for the initialization of  $\lambda_k[c]$  the bit-level extrinsic output of the turbo SISO  $\lambda_k[u]$ . These metrics are passed through the deinterleaver along with the codeword.

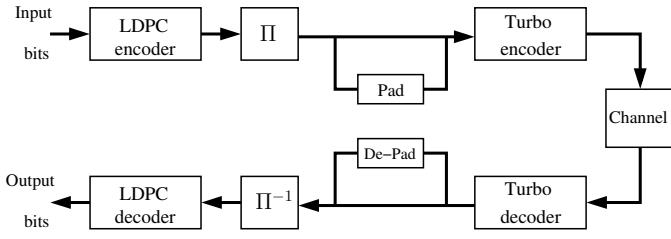


Figure 1: Serial concatenation of LDPC and turbo codes FEC scheme

The CCSDS suggests three FEC schemes for space communications in [1]: a RS-convolutional codes concatenated scheme, turbo codes and LDPC codes. Deep space communications requiring very low bit error rates address turbo codes in particular, allowing four code rates ranging from 1/6 to 1/2, and four information block lengths in the range 1784-8920. The WiMAX standard [19] relies on a wide set of Quasi-Cyclic LDPC codes (QC-LDPC), together with turbo codes of different length and rates. The two code types are mutually exclusive options in the standard: their proven effectiveness and implementation-friendly structure, however, make them ideal candidates for concatenation towards deep-space applications, regardless of the relatively low performance of WiMAX LDPC codes w.r.t. CCSDS LDPC codes. Thanks to the wide variety of available codes, it has been possible to experiment with different code combinations consisting of both WiMAX and CCSDS codes. Though CCSDS Single-Binary (SB) turbo codes employ 16 states, it is proven in Section IV that also the Duo-Binary (DB), eight-state codes used in WiMAX guarantee very good results while keeping the decoding complexity low.

#### IV. SIMULATIONS AND PERFORMANCE COMPARISONS

To evaluate the effectiveness of the proposed approach, simulations have been run on a proprietary tool. Its deeply customizable structure allows to select codes, channel model, SNR and result reliability level, together with decoding algorithms and related choices (number of iterations, stopping criteria). Moreover, it is possible to tweak a set of implementation-oriented characteristics, like different approximations of the chosen algorithms and number of bits assigned to the representation of the metrics.

In order to comply as much as possible with the requirements of CCSDS, the turbo codes suggested in [1] have been used as ICs in a first batch of simulations, and concatenated with WiMAX LDPC codes. The relatively high rate of the OC results in a concatenated rate that is very close to the CCSDS specifications. Block size compliance is guaranteed by using, if needed, multiple LDPC codewords as a single turbo information block, together with padding bits. The maximum allowed number of iterations has been set to 10 for both IC and OC decoder, and following most of the state of the art on deep space communications, the AWGN channel model has been chosen.

Moving towards a hardware implementation of the proposed FEC scheme, some limitations have been inserted in the sim-

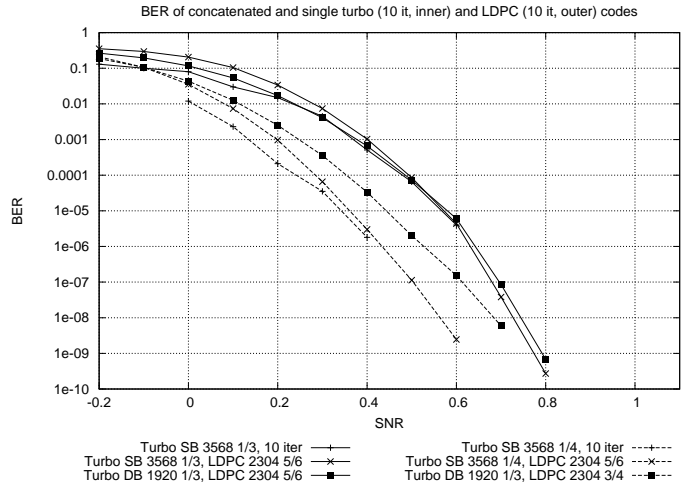


Figure 2: Concatenated LDPC and turbo BER, AWGN channel, BPSK modulation

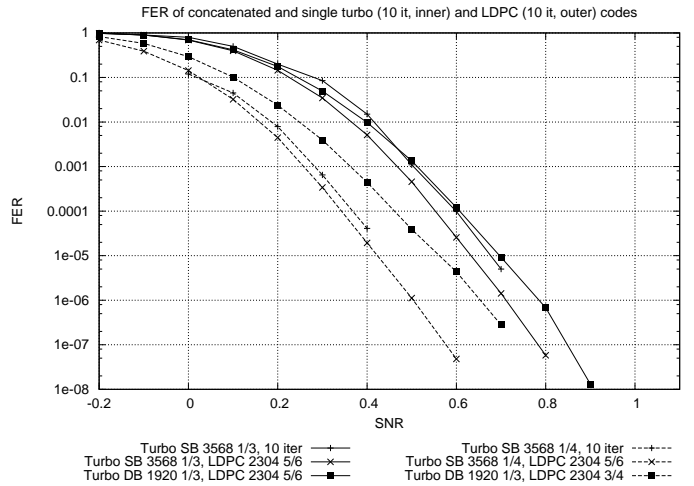


Figure 3: Concatenated LDPC and turbo FER, AWGN channel, BPSK modulation

ulation environment. To correctly evaluate the impact of soft information quantization on the BER and FER, the dynamic range of all metrics involved in the decoding process has been limited to 10 or 9 bits, with 3 bits of fractional part. For the same reason, both the LDPC and turbo codes have been decoded with the BCJR algorithm, thus leading to low decoding complexity.

Early experimentations have shown that the gain that can be obtained with the insertion of a bit interleaver between the two encoders is negligible w. r. t. the additional complexity, and it has not been considered in the plotted curve. This limited effect is mainly due to the sparse structure of the  $\mathbf{H}$  matrix, that acts as an interleaver by itself [18].

Fig. 2 and 3 plot a set of meaningful BER and FER curves respectively. The “+” marker indicates the curves provided by CCSDS in [1] for SB turbo codes of rate 1/3 (continuous) and 1/4 (dashed). They are obtained with 10 decoder iterations, QPSK modulation and AWGN channel. The x-marked curves show the performance of these codes when concatenated with a WiMAX rate 5/6 LDPC code. It can be seen that both

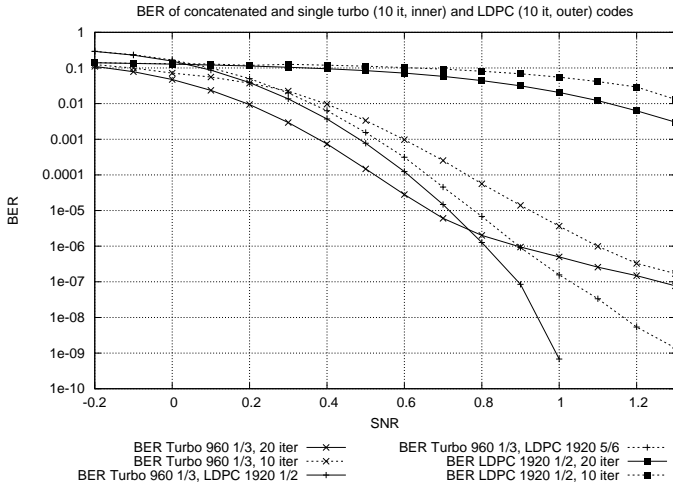


Figure 4: LDPC and DB turbo BER, concatenated and single-code, AWGN channel, BPSK modulation

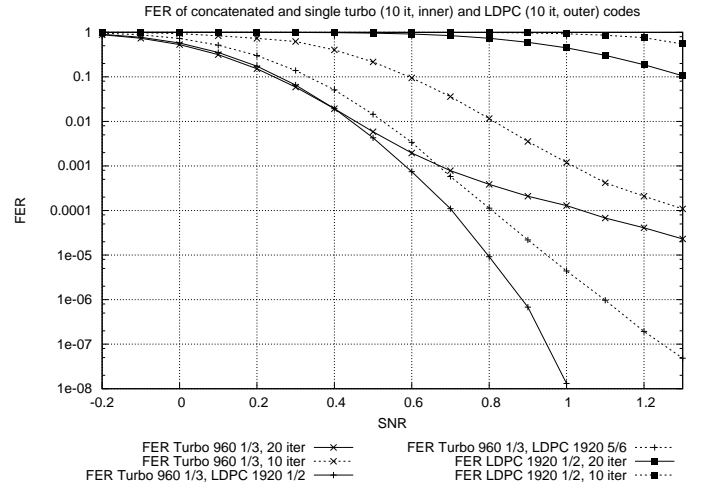


Figure 5: LDPC and DB turbo FER, concatenated and single-code, AWGN channel, BPSK modulation

concatenated BER and FER follow very closely the standard's curves: FER results are particularly encouraging, thanks to aggregated error distributions that are addressed later in this section. Moreover, plots in [1] show error floors as early as  $\text{BER}=10^{-6}$  (block length 8920): the minimum BER simulated with the concatenated scheme is slightly above  $10^{-10}$ , with no signs of error floor.

The continuous, ■-marked curves have been obtained by substituting to the SB turbo code of CCSDS in the concatenated scheme a WiMAX DB turbo code of comparable size and same rate. The difference between the two curves is negligible, while the complexity of an 8-state turbo decoder is much lower than a 16-state one, as shown in Section V.

To evaluate the influence of IC and OC respective rates on the decoding performance, a second set of simulations has been run: the IC rate has been fixed to 1/3 and by changing the OC rate it has been possible to obtain concatenated rates equal to those of CCSDS turbo codes. In both Fig. 2 and 3, the dashed, ■-marked curve has a concatenated rate of 1/4, obtained by CTC 1/3 + LDPC 3/4. It can be noticed how the lower rate of the OC fails to deliver the same BER and FER results as CTC 1/4 + LDPC 5/6: this behavior, observed also in the CTC 1/6 + LDPC 5/6 against CTC 1/3 + LDPC 1/2 case, reveals how the IC turbo rate is more critical than for the LDPC OC.

Fig. 4 plots a set of BER curves to compare the performance of WiMAX concatenated codes against single LDPC and turbo codes. The curves showing the "+" marker refer to the concatenated FEC scheme: both use a WiMAX turbo code of rate 1/3 and 960 two-bit input symbols. The continuous line has been obtained using a rate 1/2, codeword length 1920 LDPC, while the dashed one with a rate 5/6 LDPC. The higher rate LDPC results in a less steep curve: this degradation can be addressed by rising  $\text{Iter}_{in}$ , with the two curves superimposed at  $\text{Iter}_{in}=20$ . These plots are compared to the constituent rate 1/3 CTC and rate 1/2 LDPC with different numbers of allowed iterations. Since the concatenated scheme has at its disposal up to 20 iterations (10 CTC + 10

LDPC), single-code curves are plotted with both 20 and 10 iterations maximum. The concatenated BER shows very good performance at low  $E_b/N_0$ , crossing the  $10^{-6}$  threshold at  $E_b/N_0=0.9$  dB when using the rate 5/6 LDPC OC. At higher  $E_b/N_0$ , its performances are even more remarkable: a total of  $2 \cdot 10^8$  frames have been simulated for all the shown  $E_b/N_0$  points, for a total of  $1.92 \cdot 10^{11}$  information bits, and no errors were counted for  $E_b/N_0$  higher than 1.0 dB when using the rate 1/2 LDPC code. The curves show no sign of error floor and constant BER decrease. At low  $E_b/N_0$ , the 20-iterations single CTC outperforms the concatenated schemes of up to 0.15 dB: the difference is smaller than that reported in [18] with much more favorable conditions, and the crossing point occurs at a higher BER and much lower  $E_b/N_0$ .

Fig. 5 shows the FER curves for the same parameters as Fig. 4: the concatenated FER reaches very low values ( $7 \cdot 10^{-8}$  with rate 5/6 LDPC code). The difference with the 20-iteration single CTC curve at low  $E_b/N_0$  is substantially reduced (0.08 dB maximum) w. r. t. the BER, and the crossing point is moved at lower  $E_b/N_0$ . This is due to the fact that very often a failed decoding with the concatenated scheme is due to a high number of wrong bits within the same frame. Consequently, BER and FER scale differently, since errors are clustered together and affect a very low number of frames.

Table I provides a comparison of the proposed FEC scheme with similar state of the art solutions. Solution **A** refers to CCSDS SB turbo 1/4 + WiMAX LPDC 5/6, while solution **B** to CCSDS SB turbo 1/3 + WiMAX LPDC 5/6, both already shown in Fig. 2 and Fig.3. To help a fair comparison with coding schemes with different rate, the  $\Delta_{SHN}$  row identifies the distance of the BER curve from the Shannon limit at  $\text{BER}=10^{-6}$ : in both cases the distance is less than 1.5 dB. The obtained  $\Delta_{SHN}$  is similar to that of the AR4JA LDPC codes proposed by CCSDS [1], but has been obtained with a much smaller number of iterations.

In a recent work [20], a FEC scheme for 3D HDTV using an outer block turbo code (BTC) concatenated to an LDPC code is proposed. The scheme is shown to outperform the DVB-

TABLE I. PERFORMANCE COMPARISON AMONG FEC SCHEMES

	<b>A</b>		<b>B</b>		[20]	[21]	[5]	[6]	[22]	[18]	[23]
Application	Deep space		3D HDTV		Satellite	Deep space	Deep space	–	Mobile		
Inner Code	SB CTC		LDPC		NB-LDPC	QC-LDPC	LT	Parallel	SB CTC		
Outer Code	QC-LDPC		BTC		LT		NB-LDPC	RSC/LDPC	LDPC		
Rate <sub>in</sub>	1/4	1/3	1/2		2/3		25/49	1/2	1/3		
Rate <sub>out</sub>	5/6	5/6	467/500		9/10	1/3	49/50	1/2	7/8		
Rate <sub>concatenated</sub>	5/24	5/18	467/1000		3/5		1/2	1/3	7/24		
Input <sub>in</sub>	3568		16 K		1000 symbols	2379	32 K	504	2048		
Input <sub>out</sub>	1920		15 K		900 symbols		16 K	504	1792		
Inner Decoding Alg.	BCJR		BP		FFT-BP	BP	N/A	Log-MAP	BP		
Outer Decoding Alg.	BCJR		CHASE		MP			LLR-BP	Log-MAP		
Iter <sub>in</sub>	10		50		20	15	N/A	8	5	5	
Iter <sub>out</sub>	10		N/A		N/A			10	50	100	
Quantization	10-9 bits		Floating Point		Floating Point	Floating Point	Adaptive	Floating Point	Floating Point		
Channel	AWGN		Rayleigh		AWGN	AWGN	AWGN	AWGN	AWGN		
$E_b/N_0$ @ BER=10 <sup>-6</sup>	0.43	0.65	4.4		1.85	N/A	N/A	2.35	1.75	1.55	
FER @ BER=10 <sup>-6</sup>	8 · 10 <sup>-6</sup>	8 · 10 <sup>-6</sup>	4 · 10 <sup>-4</sup>		N/A	N/A	N/A	2 · 10 <sup>-5</sup>	N/A	N/A	
$\Delta_{SHN}$ @ BER=10 <sup>-6</sup>	1.38	1.43	4.50		1.55			2.90	2.43	2.23	
minimum BER	2 · 10 <sup>-9</sup>	< 10 <sup>-10</sup>	2 · 10 <sup>-7</sup>		8 · 10 <sup>-7</sup>	3 · 10 <sup>-6</sup>	N/A	1.2 · 10 <sup>-7</sup>	4 · 10 <sup>-7</sup>	2 · 10 <sup>-7</sup>	
minimum FER	6 · 10 <sup>-8</sup>	1.1 · 10 <sup>-8</sup>	8 · 10 <sup>-5</sup>		N/A	N/A	10 <sup>-8</sup>	6 · 10 <sup>-6</sup>	N/A	N/A	
$E_b/N_0$ @ min	0.6	0.9	4.6		2.0	0.3	1.05	2.5	1.9	1.6	

T2 standard serial concatenation of BCH and LDPC codes. Contrariwise to CTCs, BTCs are obtained by concatenating various BCH codes, and decoded via CHASE algorithm, whose implementation complexity is estimated comparable to that of BCJR. The BER and FER performance are greatly outperformed by this work's, with approximately 4 dB gain, and a very high  $\Delta_{SHN}$ . This could partly be due to the higher code rate and to the fading channel model, but [20] sets a very high number of iterations for the inner code, a large block size and floating point precision for the simulations, all factors that contribute to the improvement of results.

Luby Transform (LT) or fountain codes have been used together with non-binary LDPC (NB-LDPC) codes in [21] for satellite communications. The resulting system is very flexible, thanks to LT codes, and the presence of NB-LDPC codes guarantees a high error correction power even at high rates. The decoding complexity, however, suffers from the concurrent FFT-based BP and message passing algorithms, much higher than a single BCJR. The BER shows 1.2 dB loss w. r. t. solution **B**: for the same rate and precision, the two FEC systems should yield comparable results. This is confirmed by the comparable  $\Delta_{SHN}$  metrics. Both **A** and **B**, however, outperform the LT+binary LDPC codes of [24].

The QC-LDPC construction scheme for deep space communications described in [5] gives very good results without making use of concatenation: although the curves do not show low BER points, a 0.4 dB gain can be observed against the plots with similar rate in Fig. 2. These curves have been drawn with floating-point precision and a decoding algorithm devoid of approximations: some degradation of performance is consequently to be expected after the implementation. The complexity of the probability-domain BP algorithm, moreover, is very high, burdening the hypothetical hardware with large area occupation and high power consumption.

The joint source-channel coding scheme described in [6], aimed at deep space image transmission, uses Raptor codes, *i. e.* a concatenation of an LT code with a precode, in this case a

very high-rate NB-LDPC. This powerful coding scheme, also addressed in [21], obtains very good results at high coding rates: FER shows only 0.15 dB loss w. r. t. solution **B**, regardless of the rate difference.

In [22] parallel concatenation of LDPC and RSC codes is explored. The LLR-based BP algorithm implemented for the LDPC part allows good performance also with relatively small block sizes and a few allowed iterations: still, it is outperformed by **A** by 1.70 dB gain at BER=10<sup>-6</sup> and one dB smaller  $\Delta_{SHN}$ , with even more difference in the FER curves.

The two closely related works [18] and [23] implement CTCs as inner and LDPC codes as OCs, decoding them with Log-MAP and probability-domain BP algorithms respectively. The work in [23] presents the same system as [18], with the addition of a certain number of global decoder iterations that slightly improve the BER. The plotted curves show a degradation of the concatenated scheme (5+50 iterations) w. r. t. the single turbo code (5 iterations) of up to 0.3 dB that has not been observed in this work (Fig. 4). Rates are comparable to that of **B**, and they both use the AWGN channel model, while the block size of **B** is larger. Regardless of the much higher precision and number of iterations allowed in [18], **A** and **B** yield better BER and  $\Delta_{SHN}$  results, with a gain ranging from 0.90 to 1.10 dB at BER=10<sup>-6</sup>.

## V. IMPLEMENTATION COMPLEXITY

The proposed FEC scheme joins the BER of turbo codes at low  $E_b/N_0$  with that of LDPC codes at higher  $E_b/N_0$ , resulting in very steep performance curves that are well suited for deep space communications. However, concatenation is usually expensive when it comes to implementation, since decoding is required for both codes separately. Resource sharing can be attempted, but if the decoding algorithms are very different the obtained area saving are often outweighed by the additional logic required. Since LDPC and turbo codes can be decoded with the BCJR algorithm, it is possible to share a large part of the datapath. Currently, the authors

are working on a flexible and efficient decoder meeting the requirements for concatenated LDPC and turbo decoding: the decoder must be able to switch between LDPC and turbo configurations on-the-fly, in case of IC failed decoding. Partial synthesis estimations show that around 95% of the LDPC datapath can be shared with the turbo datapath. Moreover, due to the higher number of states in the trellis of turbo codes, the LDPC decoder architecture can exploit an internal level of parallelism (up to  $8\times$  in presence of 16-state turbo codes). This aspect is particularly useful in case many LDPC codewords are used as a single information block for turbo codes. Taking as an example the multi-core LDPC-turbo decoder presented in [9], a 95% shared datapath would result in a 14% area reduction in every processing element. The limited throughput requirements set by CCSDS allow to scale down the operating frequency: in **B**, a throughput of 2 Mb/s would be achieved at 8 MHz, with a huge decrease in power consumption.

BP and CHASE algorithms used in [20] are very different and, to the best of our knowledge, datapath sharing has never been considered. However, the adaptive BP proposed in [25] for BTC decoding is likely to allow at least partial resource sharing. Also in case of LT and NB-LDPC codes used in [21] and [6], while the datapaths are different, both decoding processes rely on a bipartite graph: this can lead to some degree of sharing of the internal connections and memories.

In [22] LDPC decoding is performed through LLR-BP: the min-sum approximation only requires sums and minimum extractions, making its implementation very simple. In [26] resource sharing between min-sum and SISO-based turbo decoding is considered, resulting in unsatisfying improvements: the overhead would be even greater with the probability-domain BP used in [18].

## VI. CONCLUSION AND FUTURE WORK

In this paper, a FEC scheme relying on serial concatenation of parallel CTCs and LDPC codes is presented. Detailed simulations and comparison with the state of the art show competitive results, outperforming or being comparable to the latest concatenation and deep space schemes. The use of the same algorithm to decode both codes leads to a small area, low power implementation that is currently under development. Early complexity estimations show that it is possible to implement the proposed approach at a very small cost w. r. t. even single code deep space communications FEC schemes.

## REFERENCES

- [1] *TM Synchronization and Channel Coding - Summary of Concept and Rationale*, Consultative Committee for Space Data Systems (CCSDS) Std. 130.1-G-2, Nov. 2012.
- [2] *TM Channel Coding Profiles*, Consultative Committee for Space Data Systems (CCSDS) Std. 131.4-M-1, Jul. 2011.
- [3] C. Berrou, A. Glavieux, and P. Thitimajshima, "Near Shannon limit error correcting coding and decoding: Turbo codes," in *IEEE International Conference on Comm.*, 1993, pp. 1064–1070.
- [4] R. G. Gallager, "Low density parity check codes," *IRE Transactions on Information Theory*, vol. IT-8, no. 1, pp. 21–28, Jan 1962.

- [5] N. Andreadou, F.-N. Pavlidou, S. Papaharalabos, and P. Mathiopoulos, "Quasi-cyclic low-density parity-check (QC-LDPC) codes for deep space and high data rate applications," in *Satellite and Space Communications, 2009. IWSSC 2009. International Workshop on*, sept. 2009, pp. 225–229.
- [6] O. Bursalioglu, G. Caire, and D. Divsalar, "Joint source-channel coding for deep space image transmission using rateless codes," in *Information Theory and Applications Workshop (ITA), 2011*, feb. 2011, pp. 1–10.
- [7] Z. Wang and Z. Cui, "Low-complexity high-speed decoder design for Quasi-Cyclic LDPC codes," *Very Large Scale Integration (VLSI) Systems, IEEE Transactions on*, vol. 15, no. 1, pp. 104–114, jan. 2007.
- [8] A. Ahmed, M. Awais, A. ur Rehman, M. Maurizio, and G. Masera, "A high throughput turbo decoder VLSI architecture for 3GPP LTE standard," in *Multitopic Conference (INMIC), 2011 IEEE 14th International*, dec. 2011, pp. 340–346.
- [9] C. Condo, M. Martina, and G. Masera, "VLSI implementation of a multi-mode turbo/LDPC decoder architecture," *Circuits and Systems I, IEEE Transactions on*, to appear.
- [10] M. Alles, T. Vogt, and N. Wehn, "FlexiChaP: A reconfigurable ASIP for convolutional, turbo, and LDPC code decoding," in *Turbo Codes and Related Topics, 2008 5th International Symposium on*, 2008, pp. 84–89.
- [11] L. R. Bahl, J. Cocke, F. Jelinek, and J. Raviv, "Optimal decoding of linear codes for minimizing symbol error rate," *IEEE Transactions on Information Theory*, vol. 20, no. 3, pp. 284–287, Mar 1974.
- [12] S. Papaharalabos, P. T. Mathiopoulos, G. Masera, and M. Martina, "On optimal and near-optimal turbo decoding using generalized max\* operator," *IEEE Comm. Letters*, vol. 13, no. 7, pp. 522–524, Jul 2009.
- [13] D. Hocevar, "A reduced complexity decoder architecture via layered decoding of LDPC codes," in *Signal Processing Systems, IEEE Workshop on*, 2004, pp. 107–112.
- [14] M. Fossorier, M. Mihaljevic, and H. Imai, "Reduced complexity iterative decoding of low-density parity check codes based on belief propagation," *IEEE Trans. on Comm.*, vol. 47, no. 5, pp. 673–680, May 1999.
- [15] M. Mansour and N. Shanbhag, "Turbo decoder architectures for low-density parity-check codes," in *Global Telecommunications Conference, 2002. GLOBECOM '02. IEEE*, vol. 2, nov. 2002, pp. 1383–1388 vol.2.
- [16] M. Martina, G. Masera, S. Papaharalabos, P. T. Mathiopoulos, and F. Gioulekas, "On practical implementation and generalizations of max\* operator for turbo and LDPC decoders," *IEEE Transactions on Instrumentation and Measurement*, vol. 61, no. 4, pp. 888–895, Apr 2012.
- [17] *Radio Frequency and Modulation Systems Part 1: Earth Stations and Spacecraft*, Consultative Committee for Space Data Systems (CCSDS) Std. 401.0-B-21, Jul. 2011.
- [18] S. H. Lee, J. A. Seok, and E. K. Joo, "Serial concatenation of LDPC and turbo code for the next generation mobile communications," in *Wireless and Optical Communications Networks, 2005. WOCN 2005. Second IFIP International Conference on*, march 2005, pp. 425–427.
- [19] *IEEE Standard for Local and Metropolitan Area Networks Part 16*, IEEE Std 802.16e-2005 Std., 2006.
- [20] K. Kwon, H. H. Im, and J. Heo, "An improved FEC system for next generation terrestrial 3D HDTV broadcasting," in *Consumer Electronics (ICCE), 2012 IEEE International Conference on*, jan. 2012, pp. 327–328.
- [21] W. Lei, L. Jing, and W. J. bo, "Design of concatenation of fountain and non-binary LDPC codes for satellite communications," in *Information Engineering and Computer Science (ICIECS), 2010 2nd International Conference on*, dec. 2010, pp. 1–4.
- [22] S. Gounai, T. Ohtsuki, and T. Kaneko, "Performance of concatenated code with LDPC code and RSC code," in *Communications, 2006. ICC '06. IEEE International Conference on*, vol. 3, june 2006, pp. 1195–1199.
- [23] S. H. Lee, J. A. Seok, and E. K. Joo, "Serially concatenated LDPC and turbo code with global iteration," in *Systems Engineering, 2005. ICSEng 2005. 18th International Conference on*, aug. 2005, pp. 201–204.
- [24] W. Yao, L. Chen, H. Li, and H. Xu, "Research on fountain codes in deep space communication," in *Image and Signal Processing, 2008. CISP '08. Congress on*, vol. 2, may 2008, pp. 219–224.
- [25] C. Jego and W. Gross, "Turbo decoding of product codes using adaptive belief propagation," *Communications, IEEE Transactions on*, vol. 57, no. 10, pp. 2864–2867, october 2009.
- [26] J. Dielissen, N. Engin, S. Sawitzki, and K. van Berkel, "Multistandard FEC decoders for wireless devices," *Circuits and Systems II, IEEE Transactions on*, vol. 55, no. 3, pp. 284–288, march 2008.